

Optics Letters

On a universal solution to the transport-of-intensity equation

JIALIN ZHANG,^{1,2,3}  QIAN CHEN,^{1,2,5}  JIASONG SUN,^{1,2,3}  LONG TIAN,^{4,6} AND CHAO ZUO^{1,2,3,7} 

¹School of Electronic and Optical Engineering, Nanjing University of Science and Technology, No. 200 Xiaolingwei Street, Nanjing, Jiangsu 210094, China

⁴School of Science, Nanjing University of Science and Technology, No. 200 Xiaolingwei Street, Nanjing, Jiangsu 210094, China

²Jiangsu Key Laboratory of Spectral Imaging and Intelligent Sense, Nanjing, Jiangsu 210094, China

³Smart Computational Imaging Laboratory (SCILab), Nanjing University of Science and Technology, Nanjing, Jiangsu Province 210094, China

⁵e-mail: chenqian@njust.edu.cn

⁶e-mail: tianlong19850812@163.com

⁷e-mail: zuochao@njust.edu.cn

Received 16 March 2020; revised 29 May 2020; accepted 31 May 2020; posted 1 June 2020 (Doc. ID 391823); published 29 June 2020

The transport-of-intensity equation (TIE) is one of the most well-known approaches for phase retrieval and quantitative phase imaging. It directly recovers the quantitative phase distribution of an optical field by through-focus intensity measurements in a non-interferometric, deterministic manner. Nevertheless, the accuracy and validity of state-of-the-art TIE solvers depend on restrictive pre-knowledge or assumptions, including appropriate boundary conditions, a well-defined closed region, and quasi-uniform in-focus intensity distribution, which, however, cannot be strictly satisfied simultaneously under practical experimental conditions. In this Letter, we propose a universal solution to TIE with the advantages of high accuracy, convergence guarantee, applicability to arbitrarily shaped regions, and simplified implementation and computation. With the “maximum intensity assumption,” we first simplify TIE as a standard Poisson equation to get an initial guess of the solution. Then the initial solution is further refined iteratively by solving the same Poisson equation, and thus the instability associated with the division by zero/small intensity values and large intensity variations can be effectively bypassed. Simulations and experiments with arbitrary phase, arbitrary aperture shapes, and nonuniform intensity distributions verify the effectiveness and universality of the proposed method. © 2020 Optical Society of America

<https://doi.org/10.1364/OL.391823>

The transport of intensity equation (TIE) is a powerful tool for phase retrieval and quantitative phase imaging (QPI) [1]. Over the past decades, this method has attracted much attention due to its unique advantages over interferometric approaches, such as being deterministic, non-interferometric [2], applicable to temporally/spatially coherent beams, phase-unwrapping-free, and stable to environmental disturbances. It has been used widely over a wide range of light and electron beams in

numerous applications, e.g., x-ray diffraction [3], transmission electron microscopy [4], and optical QPI [5].

TIE is a second-order elliptic partial differential equation that describes the quantitative relationship between quantitative phase and intensity variation along the propagation direction. The “well-posedness” and “uniqueness” of the solution require a strictly positive intensity and, more importantly, the precise knowledge of (Dirichlet, Neumann) boundary conditions [6], which, however, are difficult to measure or to know *a priori*. For example, to obtain the Dirichlet boundary condition, one needs to know the phase values at the region boundary [1] or manually select the “smooth region” inside the phase distribution [7]. The fast Fourier transform (FFT)-based solver [2] can be used to avoid the complexity of obtaining such boundary conditions, but it assumes that the finite signal is periodic and repetitive. Nevertheless, this situation is rather restrictive and does not reflect general experimental conditions. When the actual experimental situation violates those imposed assumptions, e.g., objects located at the image borders, severe boundary artifacts will appear, seriously affecting the accuracy of the phase reconstruction [8]. On the other hand, for certain phase functions (such as tilt, defocus, and astigmatism), the defocus-induced intensity derivative signals are all concentrated at the boundary region. If the boundary conditions are not considered, the phase can never be recovered correctly.

The key to solving the above-mentioned issues is obtaining the boundary values, especially in practical experimental conditions. Zuo *et al.* [8] found that around the introduced aperture edge, the inhomogeneous Neumann boundary conditions can be obtained directly, and then TIE can be effectively and efficiently solved using the fast discrete cosine transform (DCT) with a rectangular aperture. But this solution is available only for a rectangular aperture because the DCT applies only to rectangular domains. But in practice, it is quite challenging to add an exactly rectangular aperture because of the difficulties in aperture fabrication and system alignment, or the other existing

pupils may obstruct the system aperture to be rectangular [9]. Besides the difficulties in obtaining boundary conditions, the low-frequency artifacts [10] and phase discrepancy [11] resulting from Teague's assumption are also notorious problems for the phase retrieval based on TIE. Though several iterative TIE algorithms have been proposed to compensate for the phase discrepancy and they do work under certain conditions [9,12,13], there is no theoretical guarantee for the convergence. When significant intensity variations or intensity singularities (small intensity values) exist, the iterations will become unstable and prone to divergence [12].

From the above, we know that the accuracy and validity of state-of-the-art TIE solvers depend on restrictive pre-knowledge or assumptions, including appropriate boundary conditions, a well-defined closed region, and quasi-uniform in-focus intensity distribution, which, however, cannot be strictly satisfied simultaneously under practical experimental conditions. Ideally, there are at least four issues that need to be addressed for a desired TIE solver. 1) It should account for inhomogeneous boundary conditions with experimentally measured boundary signal. 2) It should be applicable to arbitrarily shaped apertures with an arbitrarily distributed intensity function (hard/soft aperture, large intensity variations, and small intensity values). 3) It should provide accurate solution without phase discrepancy. 4) It should be efficient and strictly convergent (if it is iterative). Based on these considerations, we propose a universal solution to TIE (US-TIE) with the advantages of high accuracy, convergence guarantee, applicability to arbitrarily shaped regions, and simplified implementation and computation. Let us first start with the TIE originally proposed by Teague [1]:

$$-k \frac{\partial I(\mathbf{r})}{\partial z} = \nabla \cdot [I(\mathbf{r}) \nabla \phi(\mathbf{r})], \quad (1)$$

where $I(\mathbf{r})$ is the in-focus intensity, \mathbf{r} is the 2D spatial coordinates, $\phi(\mathbf{r})$ is the phase distribution to be solved, and k is the wave number. To simplify Eq. (1), Teague [1] suggested to introduce an auxiliary function $\psi(\mathbf{r})$ such that $\nabla \psi(\mathbf{r}) = I(\mathbf{r}) \nabla \phi(\mathbf{r})$. Then Eq. (1) can be simplified into two standard Poisson equations:

$$-k \frac{\partial I(\mathbf{r})}{\partial z} = \nabla^2 \psi(\mathbf{r}), \quad (2)$$

$$\nabla \cdot [I(\mathbf{r})^{-1} \nabla \psi(\mathbf{r})] = \nabla^2 \phi(\mathbf{r}), \quad (3)$$

which can be solved with the use of FFT [2] or DCT [8] efficiently. The solution can be simply denoted as

$$\phi(\mathbf{r}) = -k \nabla^{-2} \left\{ \nabla \cdot \left\{ \frac{1}{I(\mathbf{r})} \nabla \nabla^{-2} \left[\frac{\partial I(\mathbf{r})}{\partial z} \right] \right\} \right\}. \quad (4)$$

Equation (4) is usually referred to as the “Teague's assumption,” which suggests that the transverse flux is conservative so that it can be fully characterized by a scalar potential [1]. However, there is no guarantee that the transverse flux is always conservative due to the curl component in the Helmholtz decomposition, especially when large intensity variations or singularities exist, resulting in non-ignorable phase discrepancy [11,12]. Moreover, in experimental conditions, the intensity captured at the in-focus plane $I(\mathbf{r})$ often contains dark regions where the intensity value approaches or equals zero. This precludes the direct use of Eq. (4) for phase reconstruction since

$I(\mathbf{r})$ appears in the denominator. In fact, the “divide-by-zero” is the major factor behind the phase discrepancy and the instability of the state-of-the-art TIE solvers. Fortunately, we found that when the in-focus intensity is uniform (\tilde{I}), it can be pulled directly out of the gradient operator, and TIE directly boils down to a Poisson equation: $-k \frac{\partial I(\mathbf{r})}{\partial z} = \tilde{I} \nabla^2 \phi(\mathbf{r})$. In such a case, the transverse flux is always conservative and Teague's assumption will no longer be necessary, and thus, the solution to TIE becomes trivial and no phase discrepancy will be induced. Inspired by this observation, when solving TIE, we first assume that the in-focus image intensity is uniform with a constant value I_{\max} , where I_{\max} is the maximum value of the in-focus image intensity, to bypass the difficulties associated with the “divide-by-zero” problem. Then, the solution of the phase takes the following form:

$$\phi(\mathbf{r}) = -\frac{k}{I_{\max}} \nabla^{-2} \left[\frac{\partial I(\mathbf{r})}{\partial z} \right], \quad (5)$$

where the inverse Laplacian operator ∇^{-2} can be effectively implemented by only one pair of FFT. But it should be noted that the maximum intensity assumption I_{\max} used here is obviously “unreasonable,” and the phase calculated by Eq. (5) is usually inaccurate. Thus, the next step is to treat the inaccurate phase $\phi_0(\mathbf{r})$ as an initial solution, and substitute it back to Eq. (1). The inaccurate solution results in inconsistency between the calculated intensity derivative J_n and the real measurement value, which is treated as the error signal for another round of phase reconstruction. The solution $\phi_0(\mathbf{r})$ is also taken as the “correction term,” which is added back to $\phi_0(\mathbf{r})$ to get an updated phase estimate. This completes one iteration of the reconstruction algorithm, and the procedure is iteratively repeated until convergence as shown in Fig. 1. It should be noted that during the iterative process, the maximum intensity assumption I_{\max} is always assumed so that the solution in each iteration can be effectively implemented by two simple FFTs [instead of eight as in the conventional FFT-based TIE solver (FFT-TIE)]. Though the maximum intensity assumption I_{\max} is not physically grounded, we access the correctness of our current estimate with the original TIE, which guarantees that when the iterative algorithm converges with an insignificant error signal, the accurate solution to TIE is certain to arrive.

It should be mentioned that the universal solution proposed here is quite similar to the previous iterative algorithms for compensating for the “phase discrepancy” owing to the “Teague's assumption” [12], and solving the boundary condition problem with an arbitrarily shaped aperture [9]. The only difference is that the maximum intensity assumption I_{\max} is introduced here to simplify the solution and prevent numerical instability. More importantly, the maximum intensity assumption I_{\max} is also the key to the convergence of the iterative algorithm. The rigorous proof of convergence of iterative process can be found in Ref. [14]. In the proof, we first establish the Sobolev space $W^{2,2}$ *a priori* estimate to the solution on each step [15]. Then based on Sobolev's embedding theorem [16], we can derive that the solution on the n^{th} step is comparable to the quantity $[(I_{\max} - I)/I_{\max}]^n$. Due to the maximum intensity assumption I_{\max} , the common ratio of this geometric sequence can be constrained within the range of zero to one, which mathematically guarantees that the iterative algorithm is convergent. The convergence processes might slow down in the presence of small

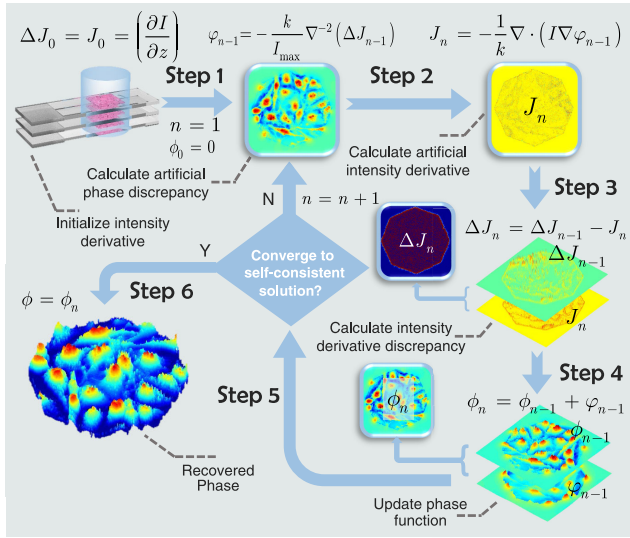


Fig. 1. Flow chart of the US-TIE method.

intensity values or intensity singularities $[(I_{\max} - I)/I_{\max} \approx 1]$, but never deviate off track.

Simulations are carried out to verify the validity and effectiveness of the proposed method. In the first simulation, an irregular hard aperture with uniform intensity distribution is used, as shown in Figs. 2(a1) and 2(a2). The phase distribution is a shifted astigmatism function defined on a 256×256 grid: $\phi(r) = 10r_x^2 - 10r_y^2 - 0.7r_x + 2r_y + 0.82$, as shown in Fig. 2(a3). Defocused images ($\Delta z = 1 \mu\text{m}$) are obtained based numerical propagation, as shown in Fig. 2(a2). US-TIE converges after 30 iterations, producing an accurate solution with negligible error (RMSE 0.0035 rad) [Figs. 2(a4) and 2(a5)]. The second simulation tests the US-TIE under soft-edged illumination. The intensity profile is a Gaussian beam within a circular aperture [Figs. 2(b1)–2(b3)]. The US-TIE, once again, successfully recovers the correct phase distribution even in the dark region, as shown in Figs. 2(b4) and 2(b5). In both cases, the FFT-TIE solver fails to produce reasonable phase reconstruction results due to the violation of periodic boundary conditions, leading to very large phase errors [Figs. 2(a6) and 2(b6)]. The iterative DCT method (Iter-DCT) can handle the cases of arbitrarily shaped apertures to a certain extent, but the residual

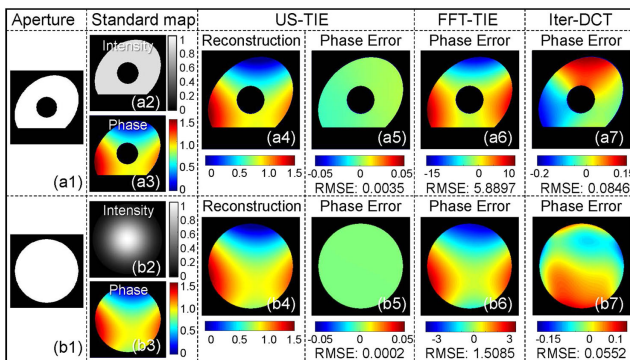


Fig. 2. Comparison of US-TIE, FFT-TIE, and Iter-DCT with irregular and soft-edged apertures. (a1), (b1) Shapes of apertures. (a2), (b2) In-focus intensities. (a3), (b3) True phases. (a4), (b4) Retrieved phases with US-TIE. (a5)–(a7), (b5)–(b7) Phase errors.

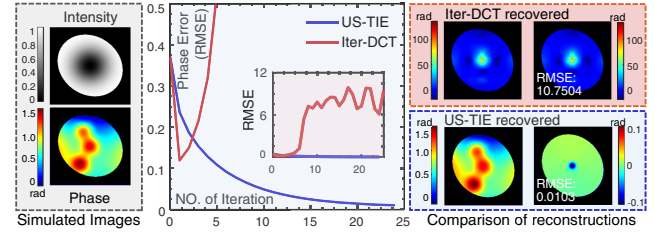


Fig. 3. Comparison between US-TIE and Iter-DCT. Left: simulated intensity and phase distribution. Middle: RMSE curves versus the iteration number. Right: reconstruction results.

phase errors are still non-negligible, as shown in Figs. 2(a7) and 2(b7).

In order to further verify the stability and convergence properties of US-TIE, we consider another challenging case of an inverse Gaussian beam (containing an intensity singularity, i.e., zero intensity value) and irregular phase distribution, as shown in the left column of Fig. 3. As the number of iterations increases, the RMSE of US-TIE drops rapidly and finally converges after 24 iterations (RMSE 0.0103 rad, total computation time 0.08s with a 3.6 GHz laptop), as shown in Fig. 3 (blue curve). Note that phase errors appear only around the intensity singularity, where the phase value is not well defined. In contrast, the RMSE curve of the Iter-DCT method rebounds after one iteration, and the iteration diverges (RMSE 10.7504 rad) due to the large phase discrepancy resulting from small intensity values (red curve). It should also be mentioned that, in addition to high accuracy and stable convergence, US-TIE improves the computational speed (~ 3.5 ms per iteration) by more than one order of magnitude compared to the Iter-DCT method (~ 36 ms per iteration) because only two FFTs are involved for each iteration.

Two experiments are performed to demonstrate the practicality of US-TIE. As illustrated in Fig. 4, an inverted bright-field microscope (Olympus IX83) attached with a $4f$ imaging system is used to acquire the in- and out-of-focus intensity images by axially translating the camera. The pixel size of the camera (The Imaging Source DMK 72BUC02, 1280×960) is $2.2 \mu\text{m}$, and the central wavelength of the illumination is 550 nm . In order to simplify the implementation, apertures (rectangle-like, octagon-like) are inserted on the intermediate image plane of the microscope instead of on the real object plane, as shown in Fig. 4. Figure 5 shows the reconstructed results of the microlens array based on the FFT-TIE [Fig. 5(b)], Iter-DCT [Fig. 5(c)], and proposed US-TIE [Fig. 5(d)]. The classical FFT-TIE solver is implemented to retrieve the phase within the rectangular region Ω only [white rectangle in Fig. 5(a)]. The profiles of microlenses at the boundary are overestimated and distorted due to the inappropriate periodic boundary conditions, as shown in Fig. 5(b). The Iter-DCT, however, produces erroneous phase reconstruction due to the divergence induced by small intensity values [dirt on the microlens and dark background; see Fig. 5(a)], as shown in Fig. 5(c). In contrast, the proposed US-TIE provides the “unbiased” solution of TIE that is free from any boundary errors and phase discrepancies. The cross-sectional profile of one individual lens [indicated in Fig. 5(d)] is shown in Fig. 5(e), which demonstrates a good accordance with the manufacturer’s specifications ($125 \pm 5\%$ rad).

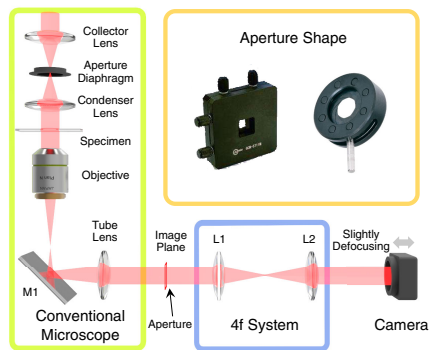


Fig. 4. Experimental setup is implemented by using an inverted bright-field microscope and a $4f$ system-based TIE module with an aperture at the image plane.

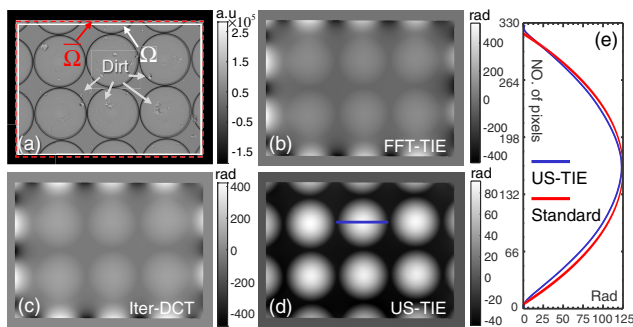


Fig. 5. (a) Initial intensity derivative. (b)–(d) Reconstructed phase distribution separately based on the classical FFT-TIE, Iter-DCT, and US-TIE methods. (e) Comparison of the reconstructed and standard phase profiles.

Finally, US-TIE is applied to QPI of live HeLa cells with an octagonal aperture. In the raw image shown in Fig. 6(a), it is observed that some cells are located across the aperture boundary. According to the intensity histogram, the aperture can be obtained by simple thresholds, and the result [Fig. 6(d)] can be recovered based on the FFT-TIE solver when the zero-value region is filled with a small constant (0.01). Though intensity zeros are fixed, FFT-TIE is still quite unstable and creates significant artifacts that degrade the whole phase reconstruction prevailing. The Iter-DCT method provides a reasonable phase estimate for the first several iterations [Fig. 6(b)]. However, the iterative process goes off track gradually, resulting in a very large background curvature superimposed on the phase of cells [Fig. 6(c)]. The phase retrieved by US-TIE is shown in Fig. 6(e), which reveals sub-cellular features such as the optically thick nucleus, transported vesicle, and Golgi apparatus. In addition, the phase at the boundary of the aperture also can be accurately recovered without any boundary artifacts perceivable, as shown in the red boxed image in Fig. 6(e).

In conclusion, a US-TIE solver is proposed for phase retrieval under nonuniform illuminations, arbitrarily shaped aperture, and inhomogeneous boundary conditions. Based on the maximum intensity assumption, TIE is iteratively solved efficiently based on the simple FFT-based Poisson solver, and the phase discrepancy problem resulting from phase discrepancy owing to the Teague's assumption can be effectively addressed. The strength

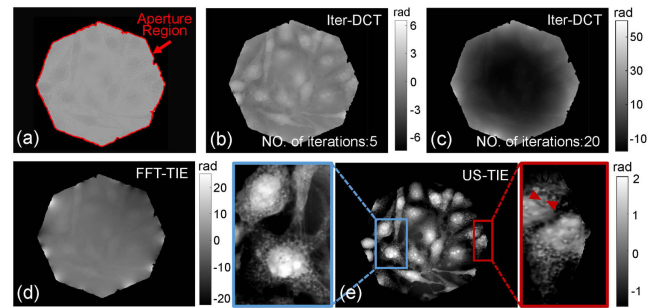


Fig. 6. (a) Intensity of the in-focus plane. Results reconstructed with the Iter-DCT solver (b), (c); FFT-TIE solver (d); and US-TIE solver (e). The blue- and red-boxed regions are zoomed for clarity.

of the proposed method lies in its high accuracy, convergence guarantee, and simple implementation, promoting broader applications of TIE in micro-optics inspection, life sciences, and bio-photonics. To aid the reader to better understand the implementation of US-TIE, we have provided the MATLAB source code and dataset for all the simulations and experiments described in this Letter in Code 1, Ref. [17].

Funding. National Natural Science Foundation of China (61722506); Leading Technology of Jiangsu Basic Research Plan (BK20192003); Outstanding Youth Foundation of Jiangsu Province of China (BK20170034); The Key Research and Development Program of Jiangsu Province (BE2017162); China Scholarship Council (201906840063).

Disclosures. The authors declare no conflicts of interest.

REFERENCES

- M. R. Teague, *J. Opt. Soc. Am.* **73**, 1434 (1983).
- D. Paganin and K. A. Nugent, *Phys. Rev. Lett.* **80**, 2586 (1998).
- K. Nugent, T. Gureyev, D. Cookson, D. Paganin, and Z. Barnea, *Phys. Rev. Lett.* **77**, 2961 (1996).
- S. Bajt, A. Barty, K. A. Nugent, M. McCartney, M. Wall, and D. Paganin, *Ultramicroscopy* **83**, 67 (2000).
- A. Barty, K. Nugent, D. Paganin, and A. Roberts, *Opt. Lett.* **23**, 817 (1998).
- T. Gureyev, A. Roberts, and K. Nugent, *J. Opt. Soc. Am. A* **12**, 1942 (1995).
- A. Parvizi, J. Müller, S. Funken, and C. Koch, *Ultramicroscopy* **154**, 1 (2015).
- C. Zuo, Q. Chen, and A. Asundi, *Opt. Express* **22**, 9220 (2014).
- L. Huang, C. Zuo, M. Idir, W. Qu, and A. Asundi, *Opt. Lett.* **40**, 1976 (2015).
- Y. Zhu, A. Shanker, L. Tian, L. Waller, and G. Barbastathis, *Opt. Express* **22**, 26696 (2014).
- J. A. Schmalz, T. E. Gureyev, D. M. Paganin, and K. M. Pavlov, *Phys. Rev. A* **84**, 023808 (2011).
- C. Zuo, Q. Chen, L. Huang, and A. Asundi, *Opt. Express* **22**, 17172 (2014).
- S. Mehrabkhani, L. Wefelnberg, and T. Schneider, *Opt. Express* **26**, 11458 (2018).
- J. Zhang, "2020_USTIE_SI," figshare (2020), https://figshare.com/articles/2020_USTIE_SI_pdf/11944968.
- R. A. Adams and J. J. Fournier, *Sobolev Spaces, Pure and Applied Mathematics* (Elsevier, 2003), Vol. **140**.
- H. Brezis, *Functional Analysis, Sobolev Spaces and Partial Differential Equations* (Springer, 2010).
- J. Zhang, "The MATLAB source code and dataset for US_TIE," figshare (2020), <https://doi.org/10.6084/m9.figshare.11984439>.